Biochimica et Biophysica Acta, 600 (1980) 108—116

BBA 78851

$(10.5\ Å)^{-1}$ DIFFRACTION AND TRANSMEMBRANE PROTEINS OF ERYTHROCYTE GHOST MEMBRANES

W. LESSLAUER

Theodor Kocher Institute, University of Berne, P.O. Box 99, CH-3000 Berne 9 (Switzerland)

(Received October 8th, 1979)

Key words: Erythrocyte membrane; Transmembrane protein; Protein conformation; Low-angle diffraction

Summary

Four types of erythrocyte ghost membrane (human ghosts, human ghosts stripped of major non-integral membrane proteins, sheep ghosts and agglutinated sheep ghosts) were studied by X-ray diffraction. Specimens of oriented and stacked membranes in an aqueous environment were used for diffraction experiments. Interferences from the membrane profile and from structures within the plane of the membrane were separated in the recorded patterns. Strongly equatorial diffraction bands at $(10.5\ Å)^{-1}$ were identified as in-plane diffraction and correlated with probable α-helical conformation of the transmembrane polypeptide chains of glycophorin and band III protein.

Introduction

A functionally important class of membrane proteins is the so-called transmembrane proteins which run across the hydrophobic membrane core and have residues exposed on either side of the membrane. Typical examples are glycoproteins such as histocompatibility antigens of lymphocytes with external receptor sites and internal links to cytoskeletal structures [1], or proteins implicated in transport functions such as the band III protein of the erythrocyte [2]. X-ray diffraction of ordered and wet ghost specimens provides information on the embedding of proteins in the erythrocyte membrane in its natural, i.e., aqueous environment. The degree of order which can be achieved in ghost specimens suitable for X-ray diffraction has been documented previously [3,4].

Materials and Methods

Human erythrocyte ghosts were prepared from freshly drawn blood stored overnight in an equal volume of Alsever's solution [5] essentially according to the method of Dodge et al. [6]. Stripped human ghosts, where the major non-integral membrane proteins were eluted by pH-manipulation, were prepared according to the method of Steck and Yu [7]. Sheep erythrocyte ghosts were prepared from blood of Grison mountain sheep as described previously [3,4] (see Fig. 1). Agglutinated sheep ghosts were obtained by agglutination with phytohemagglutinin (Difco). The agglutinin was dialyzed against $1 \cdot 10^{-2}$ M Tris-HCl (pH 7.4)/0.15 M NaCl, and 1.0 mg/ml purified sheep serum albumin was added after dialysis. The conditions were chosen such that a practically complete receptor occupancy was calculated using $K_a = 5.7 \cdot 10^6$ M^{-1} [8]. Cooperative phenomena and minor binding sites were neglected in the model of the agglutination reaction. These assumptions represent drastic simplifications. The receptors are bound in the plane of the membrane with average spacings of about 200 Å [9] and the occupancy of the first few receptor sites will largely determine the reaction conditions of the remaining open sites in their vicinity. An appreciable number of minor binding sites (probably mainly glycolipids) is present on the membrane surface. However, there is evidence from the agglutination titer of the supernatant of the final pellet and from the intensities of the agglutinin bands relative to the endogenous membrane protein bands on polyacrylamide gels that the desired complete receptor occupancy was practically achieved.

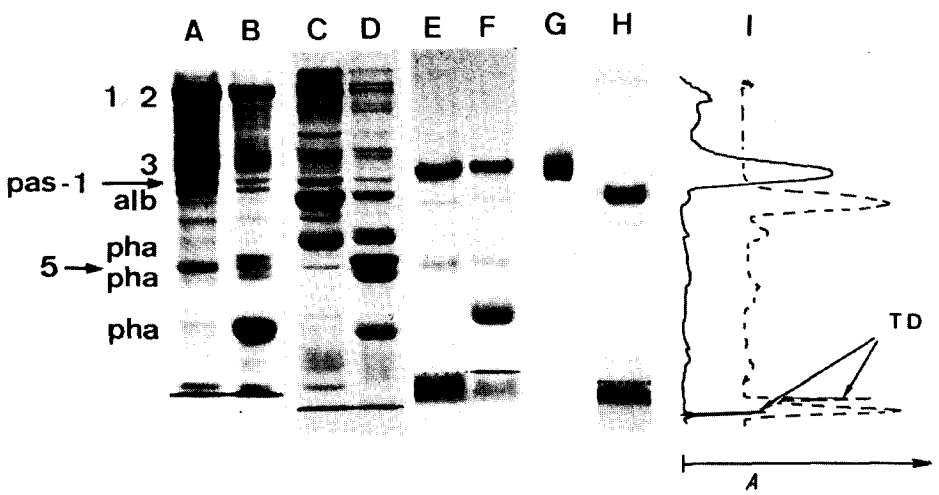

Fig. 1. 7.5% sodium dodecyl sulfate-polyacrylamide gels of the different erythrocyte ghost specimens (A,B,C,D and G are stained for protein (Coomassie brilliant blue): E,F and H are stained for carbohydrate (Periodic acid-Schiff reagent)). Numbering of bands is according to Ref. 18. pha, phytohemagglutinin bands in gels B,D and F [15]; alb, serum albumin in gels C and D; TD, tracking dye. A and E, human ghosts; B and F, human ghosts agglutinated by pha; C, sheep ghosts; D, sheep ghosts agglutinated by pha; G and H, human ghosts stripped of the major non-integral proteins [7]; I, densitometer traces of G (———) and H (- - - - -).

Sodium dodecyl sulfate-polyacrylamide gel electrophoresis was performed on slabs with a 7.5 or 13% separating gel, a 2.5% stacking gel and a discontinuous buffer system in the presence of 2% β-mercapthoethanol and 2 mM phenylmethylsulfonyl fluoride [10]. Gel patterns of the different types of ghost preparation are shown in Fig. 1.

X-ray diffraction experiments were performed as described previously [3,4]. For diffraction experiments the ghost pellets were sucked into glass capillaries of diameter 0.2—0.3 mm and 0.01 mm wall thickness. The weak shearing of the specimen in this process apparently helps to orient the membranes; well-ordered regions in the specimens are found easily by visual inspection or by observing a characteristic weak birefringence in a stereomicroscope [3]. Specimens were kept at 4.5 ± 0.2° C during exposures.

The membrane pellets after ultracentrifugation are a three-dimensional mosaic of ordered membrane stacks and of more disordered regions [3]. The stacks have dimensions comparable to the diameter of the capillaries used; their orientations are random. It is an incompletely understood observation that once the membrane pellets are transferred into the capillaries, the stacks have certain preferential orientations with respect to the coordinates of the capillaries.

The cylindrical geometry of the specimen has to be considered, if the absorption of the diffracted X-rays is evaluated (Fig. 2). For absorption corrections, only the orientation of the capillary relative to the X-ray film has to be taken into account. The magnitude of absorption corrections can be eval-

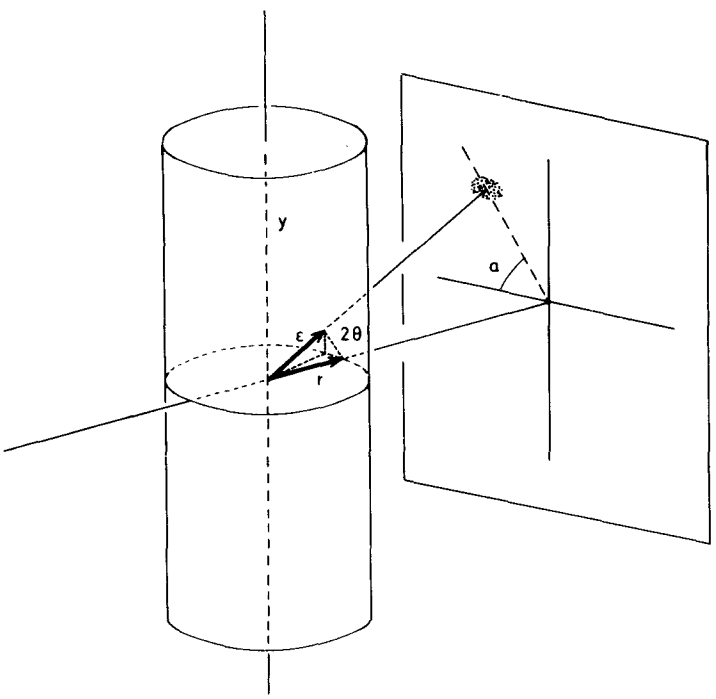

Fig. 2. Geometry of X-ray diffraction experiments.

uated in a simplified model. Diffraction is assumed to originate only in the cylinder axis. The ratio of the pathlengths in the specimen of a diffracted ray, ϵ, to that of a ray, r, diffracted in the transverse plane of the cylindrical specimen is given by:

$$\epsilon/r = (1/[\sin^2 2\,\theta\,\cos^2 t + \cos^2 2\theta])^{1/2}$$

where 2θ is the diffraction angle, t the angle between the transverse plane and the plane containing the primary beam and diffracted ray. For the $(10.5\ \text{Å})^{-1}$ diffraction, $\epsilon/r \leqslant 1.02$; for the $(3.3\ \text{Å})^{-1}$ water band $\epsilon/r \leqslant 1.12$. If the absorption of X-rays is expressed with an empirical linear absorption coefficient, μ_1, with $I = I_0 e^{-\mu_1 x}$, the absorption correction due to $\epsilon/r \geqslant 1$ can be represented by the series expansion, $1 - \mu_1 r\,(\epsilon/r - 1)$. With $\mu_1 \simeq 0.05 - 0.10\ \text{cm}^{-1}$, it becomes apparent that absorption corrections for the $(10.5\ \text{Å})^{-1}$ diffraction and for diffraction at even lower angles, $2\,\theta$, may be neglected.

The orientation of the membrane stacks in the capillaries relative to the X-ray film (irrespective of their orientation relative to the coordinates of the capillaries) is defined by the orientation of the series of reflections from the lamellar stacking which are called meridional reflections. An off-meridional angle, α, is defined: its point is on the origin of the diffraction pattern, $\alpha = 0°$ on the meridian and $\alpha = 90°$ on the equator. Densitometer traces were recorded with a Joyce-Loebl MK IIIb double-beam recording microdensitometer.

Results

Densitometer traces of the X-ray diffraction from oriented and stacked specimens of the various human and sheep erythrocyte ghost membranes are given in Fig. 3. The diffraction from all specimens is clearly separated into equatorial and meridional interferences; e.g., all patterns in Fig. 3 have a strong reflection at about $(16\ \text{Å})^{-1}$ in the meridional trace which is absent in the equatorial trace. It is, therefore, a straightforward conclusion that the membranes are oriented.

To define the meridian and equator, the axes perpendicular to the membranes are called meridional; equatorial axes lie parallel to the membranes. Several meridional low-angle reflections are observed in the various diffraction patterns; all patterns show a relatively strong reflection near $(16\ \text{Å})^{-1}$ which is resolved in the densitometer traces of Fig. 3. These reflections are explained as higher-order interferences of single lamellar repeat periods of about 160—200 Å. The highest stacking order was observed with agglutinated sheep ghosts where three strong and several weak reflections of a 180 Å period are observed [3]. These reflections are broad, but there is no significant increase in linewidth with higher-order interferences. Similar lamellar periods in the range of 160—200 Å are observed with the other ghost specimens, although the meridional reflections are less well resolved. In no instance were the typical reflections of lipid multilayer systems with periods of about 65 Å or less observed with the ghost specimens used for these experiments [4]. All ghost membranes have the strong reflection near $(16\ \text{Å})^{-1}$ (Fig. 3); a characteristic feature of the human and sheep ghost membrane thus appears to be that its transform has

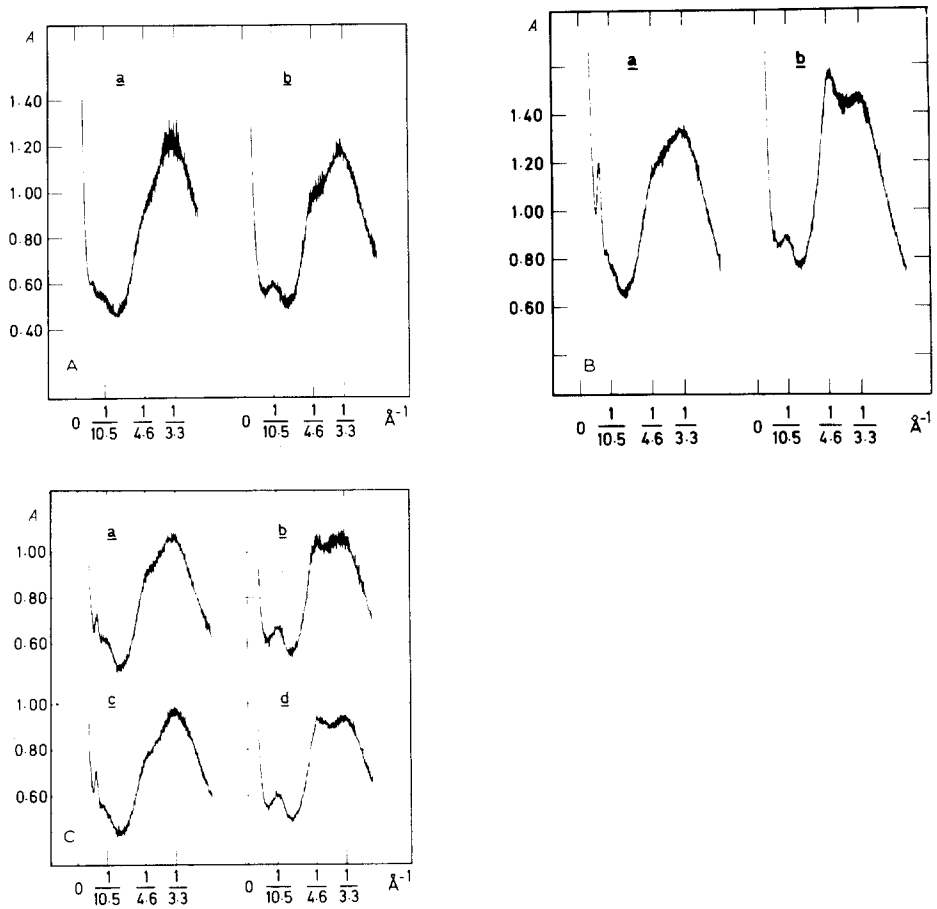

Fig. 3. Densitometer tracings of X-ray films. (A) Human ghosts, meridional (a) and equatorial (b) traces. (B) Stripped human ghosts, meridional (a) and equatorial (b) traces. (C) Sheep ghosts (a, meridional; b, equatorial) and pha-agglutinated sheep ghosts (c, meridional; d, equatorial).

large amplitudes in that region.

For the present analysis the meridional reflections are used only to define the spatial orientation of the membranes relative to the diffraction pattern; any equatorial diffraction arises from the electron density distribution in the plane of the membrane. The alignment of the membranes is not ideal. The off-meridional arcing of the lamellar reflections is an approximate measure for membrane disorientation; it was determined by measuring the radially integrated intensity of the reflections near $(16\ \text{Å})^{-1}$ as a function of the off-meridional angle α (see Fig. 4 insets). The range of α where the normalized intensity has decreased to the half maximal value is $\alpha \leqslant \pm 20^\circ$ in the experiments presented in Figs. 3 and 4. The best oriented specimens had $\alpha \simeq 12^\circ$.

The dominant equatorial diffractions are the diffraction bands at about $(10.5\ \text{Å})^{-1}$ and $(4.6\ \text{Å})^{-1}$ (Fig. 3). The $(4.6\ \text{Å})^{-1}$ band reflects the liquid-like arrangement of lipid hydrocarbon chains, although it is known that β-polypeptides also have diffraction bands near that spacing. The main interest of

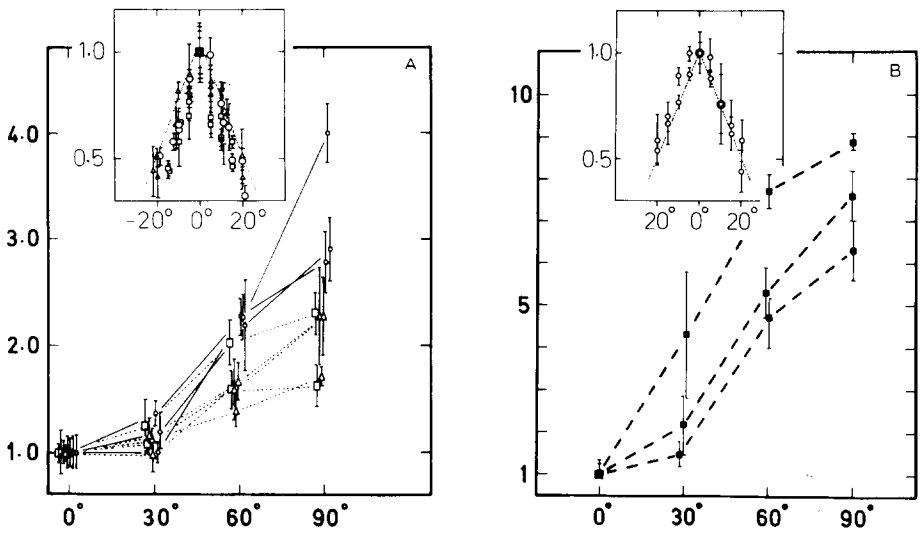

Fig. 4. Radially integrated intensity of the (10.5 Å)$^{-1}$ band as a function of the off-meridional angle α. The figure insets show the radially integrated intensity of the strong meridional reflection near (16 Å)$^{-1}$ as a function of α. (A) Human ghosts (□), sheep ghosts (△) and agglutinated sheep ghosts (○). (B) Stripped human ghosts.

this analysis is the (10.5 Å)$^{-1}$ band. The radially integrated intensity of this band as a function of α is given in Fig. 4. A region of diffuse scattering which continuously decreases from the center outwards determines the background of the (10.5 Å)$^{-1}$ region. There is no evidence that this background depends on the angle α. In the meridional trace, weak higher-order interferences of the lamellar membrane stacking reach into the (10.5 Å)$^{-1}$ region. In the equatorial trace, the low-angle slope of the (4.6 Å)$^{-1}$ band tends to fill up the high-angle minimum of the (10.5 Å)$^{-1}$ band. The baseline in the densitometer traces, therefore, was determined empirically. All traces of a given pattern were put on an absolute scale of absorbance by reference to a calibrating optical wedge. The baseline was then chosen by drawing a smooth curve through the minima on either side of the (10.5 Å)$^{-1}$ band in the meridional trace. Finally, this baseline was transferred to the other traces by matching the absorbance values of the calibrating wedge. Fig. 4 shows that the (10.5 Å)$^{-1}$ diffraction is predominantly equatorial in all human ghosts, stripped human ghosts, and native and agglutinated sheep ghosts. Furthermore, the ratio of equatorial and meridional intensities with the agglutinated sheep ghosts appears to be higher than with the native sheep ghost membranes.

In the evaluation of the densitometer traces in Fig. 3, the relative intensity scale, which is proportional to the measured absorbance values, has to be considered. The equatorial traces show a band centered at (10.5 Å)$^{-1}$ and clearly delineated by minima; in addition, the density at the Bragg's spacing of (10.5 Å)$^{-1}$ is significantly higher in the equatorial trace. This confirms that the intensity diffracted into the (10.5 Å)$^{-1}$ region is higher on the equator; the analysis of the absorbance values in the meridional and equatorial (10.5 Å)$^{-1}$ regions leads to results which are analogous to those in Fig. 4.

Discussion

The equatorial (10.5 Å)$^{-1}$ diffraction is never observed with pure lipid systems, but is well explained as diffraction from side-to-side packed α-helices or from β-sheet structures of membrane proteins. Since human ghosts stripped of the major non-integral proteins and with only glycophorin and band III protein remaining still have an equatorial (10.5 Å)$^{-1}$ band (see Figs. 3 and 4), it is concluded that polypeptide chains of these two proteins are the origin of the equatorial (10.5 Å)$^{-1}$ diffraction. Glycophorin and band III protein from biochemical data are known to be transmembrane proteins [2,11]. The anion-exchange transport function of the band III protein in some way appears related to its transmembrane configuration [12].

The alignment of the axes of these polypeptides with the normal to the membrane cannot be determined from the (10.5 Å)$^{-1}$ band, since both membrane disorientation and oblique orientation of the polypeptides across the membrane smear the (10.5 Å)$^{-1}$ band into an off-equatorial arc (Fig. 4). If the contributions to the off-equatorial smearing of the (10.5 Å)$^{-1}$ band due to membrane disorientation and to oblique orientation of polypeptides are represented as Gaussian functions of the angle, α, with integral widths, $1/w_1$ and $1/w_2$, the expected (10.5 Å)$^{-1}$ band becomes smeared into a Gaussian of integral width, $1/w = (1/w_1^2 + 1/w_2^2)^{1/2}$. Approximate values for $1/w$ and $1/w_1$ can be obtained from Fig. 4 and the inset therein. From this model it appears that membrane disorientation contributes significantly to the smearing of the observed (10.5 Å)$^{-1}$ band.

Both glycophorin and band III protein appear to occur as oligomers in the membrane [11,13] and there is further evidence that they may be grouped together [11]. Glycophorin is likely to traverse the membrane once [11]. The fragment of band III protein remaining in the membrane after proteolytic degradation from both sides of the membrane which thus appears buried in the membrane core has a molecular weight of about 17 000 [12]; it is large enough to traverse the membrane more than once. Biochemical data suggest, therefore, that there are protein islets in the membrane where several polypeptide chains traverse the membrane. Precisely such structural elements are required to satisfy the observed (10.5 Å)$^{-1}$ diffraction which, in addition, indicates that these polypeptide chains are rather well aligned perpendicular to the membrane and packed side-wise. The number of peptide chains in such a group cannot be decided from the line-width of the (10.5 Å)$^{-1}$ band, since nothing is known about the lattice of the chain packing; it is quite likely that the (10.5 Å)$^{-1}$ band is the envelope of a number of overlapping reflections in the (10 Å)$^{-1}$ region.

In principle, both α-helix and β-sheet structures of proteins have equatorial diffraction bands near (10 Å)$^{-1}$; this is well established in fiber diffraction of various polypeptides [14]. The equatorial (10.5 Å)$^{-1}$ band of the ghost membranes alone, therefore, does not establish α-helix or β-sheet structures of the membrane proteins. Additional diffraction maxima of α-helix or β-sheet structures which might resolve this ambiquity are known from fiber diffraction [14]. Of these interferences a meridional (1.5 Å)$^{-1}$ reflection has been recorded with agglutinated sheep ghosts [4], which leaves little doubt that α-helices

running across the membrane and packed side-to-side are part of the structure of those membranes, since the agglutinin itself has little or no α-helix content (Ref. 15 and Zahler, P., personal communication). This conclusion might be generalized by analogy to the non-agglutinated human and sheep ghost membranes in Fig. 3. Repeated attempts to reproduce the $(1.5\ \text{Å})^{-1}$ reflection with these specimens in Fig. 3 have failed. The reason might be that the general order is lower in those specimens; several interferences overlap in the $(1.5\ \text{Å})^{-1}$ region (the liquid scattering curves of the hydrocarbon chains of the membrane lipids [16] and of water have secondary maxima near $(1.5\ \text{Å})^{-1}$) so that any $(1.5\ \text{Å})^{-1}$ reflection would have to be quite sharp and strong in order to be recognized against this background. Axial reflections near $(5\ \text{Å})^{-1}$ are expected to be broad and weak, unless the α-helices were stacked in register through the membranes, which is unlikely. Intuitively, α-helices of hydrophobic amino acids are easily integrated in the hydrophobic membrane core; the link of the equatorial $(10.5\ \text{Å})^{-1}$ band with transmembrane proteins might be considered further evidence for α-helical structure. Isolated and solubilized band III protein from spectroscopic studies has a sizeable α-helix content [19]. However, β-sheet structures or a combination of α-helices and β-sheets cannot be excluded entirely, especially for the human erythrocyte membrane. Any additional diagnostic X-ray interference for a β-structure might be missed, the $(7.0\ \text{Å})^{-1}$ reflection for its weakness and the $(4.7\ \text{Å})^{-1}$ reflections, because they overlap with other stronger interferences.

The analysis of the relative intensities of the $(10.5\ \text{Å})^{-1}$ diffraction from different ghost specimens has to take into account disorder of polypeptide packing and membrane disorientation. With the stripped human ghosts (Figs. 3B and 4B), at least a partial aggregation of intramembrane particles might occur; if true, this could also influence the $(10.5\ \text{Å})^{-1}$ band intensity. Due to membrane disorientation, the reciprocal lattice points of a given interference order are spread into a cap in three-dimensional reciprocal space. The lamellar reflections represent a cross-section of the sphere of reflection with this cap and reflect membrane disorientation in one dimension. In principle, the spatial membrane disorientation could be measured (e.g., from rocking curves in two dimensions [17]), but the short lifetimes of the specimens exclude multiple exposures [4]. A precise knowledge of membrane disorientation would help to evaluate the significance of the $(10.5\ \text{Å})^{-1}$ band of agglutinated and non-agglutinated membranes. The present results do not allow exclusion of the possibility that structural rearrangements occur in the ghost membranes upon agglutination.

Acknowledgement

The financial support is by the Swiss National Science Foundation.

References

1 Walsh, F.S. and Crumpton, M.J. (1977) Nature 269, 307—311
2 Cabantchik, Z.I., Knauf, P.A. and Rothstein, A. (1978) Biochim. Biophys. Acta 515, 239—302
3 Lesslauer, W. (1976) Biochim. Biophys. Acta 436, 25—37
4 Lesslauer, W. (1978) Biochim. Biophys. Acta 510, 264—269

5 Kent, J.F., Bukantz, S.C. and Rein, C.R. (1946) J. Immunol. 53, 37—50
6 Dodge, J.T., Mitchell, C. and Hanahan, D.J. (1963) Arch. Biochem. Biophys. 110, 119—130
7 Steck, T.L. and Yu, J. (1973) J. Supramol. Struct. 1, 220—232
8 Kornfeld, S. and Kornfeld, R. (1971) in Glycoproteins of Blood Cells and Plasma (Jamieson, G.A. and Greenwalt, T.J., eds.), pp. 50—67, Lippincott, Philadelphia
9 Elgsaeter, A. and Branton, D. (1974) J. Cell Biol. 63, 1018—1030
10 Maizel, J.V. (1971) in Methods in Virology (Maramorosch, K. and Koprowski, H., eds.), pp. 179—246, Academic Press, New York
11 Marchesi, V.T., Furthmayr, H. and Tomita, M. (1976) Ann. Rev. Biochem. 45, 667—698
12 Grinstein, S., Ship, S. and Rothstein, A. (1978) Biochim. Biophys. Acta 507, 294—304
13 Wang, K. and Richards, F.M. (1974) J. Biol. Chem. 249, 8005—8018
14 Dickerson, R.E. (1964) in The Proteins (Neurath, H., ed.), Vol. II, pp. 671—778, Academic Press, New York
15 Miller, J.B., Hsu, R., Heinrikson, R. and Yachnin, S. (1975) Proc. Natl. Acad. Sci. U.S.A. 72, 1388—1391
16 Stewart, G.W. (1928) Phys. Rev. 31, 174—179
17 Yeager, M.J. (1975) Brookhaven Symp. Biol. 27, 77—105
18 Fairbanks, G., Steck, T.L. and Wallach, D.H.F. (1971) Biochemistry 10, 2606—2617
19 Holzwarth, G., Yu, J. and Steck, T.L. (1976) J. Supramol. Struct. 4, 161—168